Evaluation of the residual life and mechanical properties of steels with a heterophase structure

Cite as: AIP Conference Proceedings **2176**, 030016 (2019); https://doi.org/10.1063/1.5135140
Published Online: 19 November 2019

V. P. Shveikin

Evaluation of the Residual Life and Mechanical Properties of Steels with a Heterophase Structure

V. P. Shveikin[1, 2]

[1]*Institute of Engineering Science, Ural Branch of the Russian Academy of Sciences, 34 Komsomolskaya St., Ekaterinburg, 620049, Russia*
[2]*B. N. Yeltsin Ural Federal University, 19 Mira St., Ekaterinburg, 620002, Russia*

Corresponding author: shveikin60@mail.ru

Abstract. When a decision is made about prolongation of the safe service life of a critical facility above specified, measures are taken to diagnose its health and to determine its residual life. Evaluation of the residual life of critical facilities is a complex engineering problem; to solve it, one needs to have the results of a complex study of loading conditions and forms, mechanical characteristics, stress-strain state features, the presence of process defects and service-induced. The aim of this study is to create experimental methods for evaluating the residual life of critical facilities. To do this, we develop a model of degradation of the mechanical and physical properties of materials under a complex stress state and thermal action which correspond to the actual service conditions of a facility. In order to judge whether it is possible to prolong the service life of facilities, a full-scale investigation of their functional abilities is performed on the basis of studying the structure and physical-mechanical properties of a limited number of samples from one batch at the moment of investigation and a prediction is made with the use of the developed degradation model.

INTRODUCTION

Due to their high ductility and low yield stress, two-phase ferrite-martensite steels (TFMS) were first used for products made by cold forming (die-forging, extrusion, etc.) [1–3]. Studying the possibility of intentionally increasing the strength characteristics by controlling the amount and properties of the strengthening phase (martensite, bainite) with the preservation of the required level of viscoplastic characteristics due to soft ferrite has shown good prospects of using heterophase low-carbon steels instead of ferrite-pearlite ones as structural materials. Particularly, they are currently used for the production of high-strength gas and oil pipes, sheets, and strips [3–5, 8, 9].

MATERIALS AND RESEARCH METHODS

The heterophase state can be formed in the following ways:

- alloying of steels by elements increasing the stability of overcooled austenite (Mo, Cr, Ni), which makes the steels more expensive;
- accelerated cooling after rolling or furnace heating;
- heating into the intercritical temperature interval followed by cooling with a specified rate.

This section describes a new method for creating TFMS, namely stepwise quenching including heating to a temperature close to Ac_3 to form austenite inhomogeneous in carbon content, overcooling to below Ar_1 with optimum soaking, during which the necessary portion of excess ferrite precipitates, and carburization of undecomposed austenite transforming into martensite and bainite during water quenching.

Mechanics, Resource and Diagnostics of Materials and Structures (MRDMS-2019)
AIP Conf. Proc. 2176, 030016-1–030016-7; https://doi.org/10.1063/1.5135140
Published by AIP Publishing. 978-0-7354-1923-0/$30.00

Stepwise quenching, as well as heating into the intercritical temperature interval, allows one to control the amount of soft and lamellar excess ferrite and the strengthening phase (martensite + bainite), to prevent pearlite precipitations and, as a result, to obtain a predictable high complex of mechanical properties of steels.

The steels had an initial ferrite-pearlite structure resulting from normalization from 900 °C. Strip-shaped specimens sized 5.5×10×280 mm were heat-treated in a SNOL 2.3.1,5/10 oven. Some specimens were heated to a temperature of 900 or 860 °C and water-quenched after 30 min soaking. The other specimens, after austenization at the same temperatures, were overcooled to 680 °C with soaking of different durations and water-quenched.

To examine the microstructure, we used an Olympus GX-51 light-optical microscope. The microsections were etched in a 4% solution of nitric acid in ethanol.

Vickers hardness testing was performed according to GOST 9013-59. The 5.5×10×280 mm flat strips were tested for tension at a rate of 10^{-3} s^{1} in an Instron machine. The force stress was measured by a strain gauge with a maximum force of 50 kN.

The X-ray diffraction analysis was performed by means of a Bruker Advance D8 diffractometer in $K\alpha$ Cu radiation with the use of a monochromator. $K\alpha_1$ lines were isolated and the crystal lattice period was precisely determined by the programs available in the diffractometer computer. Specimens made of the same steel, normalized from 900 °C, were used as reference specimens. The degree of martensite tetragonality c/a and carbon content ρ (wt%) in martensite [13, 14] were determined by the tetragonal duplet (110)-(011+101) as

$$c/a = 1+0.0467\rho \quad (1)$$

SELECTION OF HEAT TREATMENT CONDITIONS

Austenization temperature makes a special contribution to obtaining a heterophase ferrite-martensite structure responsible for the complex of mechanical properties. Investigations have shown that, after austenization at 900 °C, overcooling to 680 °C followed by quenching, the steel hardness did not reach the desirable level and that it amounted to about at most 200 HV, although the acicular constituent amounted to ~50% in the structure. This is attributable to lower martensite hardness (strength), which is proportional to the carbon content [8, 7, 20].

After austenization at T_a = 860 °C, overcooling to T_{oc} = 680 °C and water quenching, the steel hardness notably increased and proved to be fairly sensitive to the duration of soaking under overcooling (Fig. 1). This must be due to the appearance of different amounts of high-carbon martensite from the carbon-rich regions of austenite that has formed from pearlite at low-temperature austenization [6, 10, 17, 19], as well as with the precipitation of excess ferrite [6, 7, 16, 18, 21].

The overcooling temperature was chosen from the consideration that, for T_{oc}=680 °C, the following is observed:

- considerable incubation time and low precipitation rate of excess ferrite, which allows its amount to be easily dosed;
- extremely long incubation time of pearlite precipitation, which guarantees its absence in the structure;
- high diffusive mobility of carbon atoms, which go into the bulk of undecomposed austenite from various grains of excess ferrite.

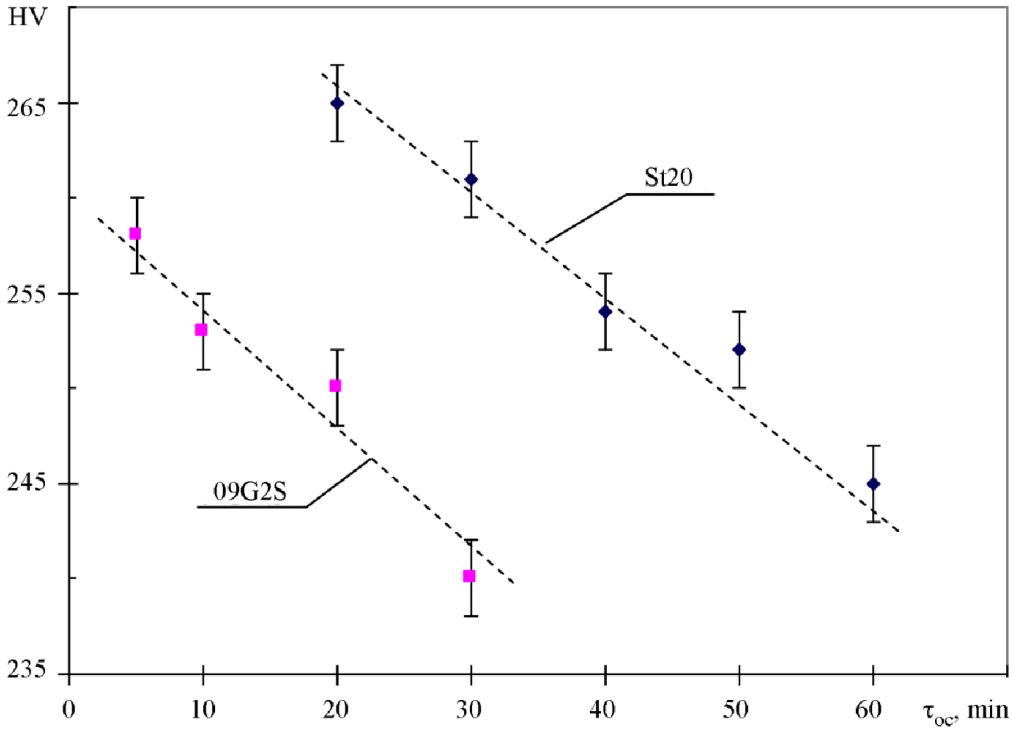

FIGURE 1. Effect of soaking duration under overcooling to 680 °C on the hardness of the St20 and 09G2S steels after stepwise quenching

However, the soaking time under overcooling τ_{oc} must be different for the steels under study since the 09G2S steel, due to lower carbon content and silicon alloying, demonstrates lower incubation time of austenite decomposition in step I than the St20 steel [6].

It is obvious from Fig. 1 that the hardness of the 09G2S steel after the same τ_{oc} is lower than that of the St20 steel and that it has a steeper behavior. This is what determined the soaking times of 5 and 20 minutes, respectively, for the 09G2S and St20 steels, and they were subsequently used in the heat treatment of the specimens in order to study the microstructure and mechanical properties.

MICROSTRUCTURE FEATURES AND MECHANICAL PROPERTIES

The metallographic examination has shown (Fig. 2a) that the microstructure of both steels after stepwise quenching consists of light-colored grains of excess ferrite sized 20 to 50 μm, contacting among themselves, and open roundish "grains" sized 10 to 30 μm, inside which acicular martensite and bainite crystals have formed. The area of the "grains" of the strengthening phase is 40 to 50%.

Electron microscopic studies of thin St20 steel foils enable these conclusions to be made more specific. In excess martensite grains with curved boundaries there is increased dislocation density, a little higher near acicular crystals of the α-phase (Fig. 2b).

Martensite of two morphological types is detected. The type I martensite crystals contain so high dislocation density ($\sim 1 \cdot 10^{11}$ sm^{-2}) that some dislocations remain intact. They have a shape of battens, ~1 μm thick, sometimes bundled (Fig. 2c). This type of martensite is typical of medium-carbon steels [7, 11, 12].

Wide plates of martensite with packs of parallel ~100 Å (10 nm) thick microtwins are typical of high-carbon martensite (Fig. 2d).

The battens of the α-phase with cementite precipitates in the form of identically oriented cementite particles are interpreted as lower bainite (Fig. 2c). The width of such battens with several curved boundaries reaches ~3 μm. 50мкм

The analysis of the ring electron diffraction patterns obtained from the entire object area irradiated by electrons has shown the presence of residual austenite.

Thus, the electron microscopy data testify that, side by side with ferrite, in the low-carbon steel after stepwise quenching there is a spectrum of shear transformation products forming one by one as the temperature decreases in the austenite regions becoming richer and richer in carbon.

The X-ray diffraction analysis has shown the distinctness of the structure of the specimens that have undergone stepwise quenching and the difference of its characteristics from those of the specimens after direct quenching.

In the X-ray diffraction patterns of the specimens directly quenched after austenization from 860 and 900 °C, the 110 line has a strictly symmetrical profile enabling us to speak about the absence of experimentally detected martensite tetragonality. At the same time, the martensite lattice period exceeds by 0.0012 Å (0.012 nm) the ferrite lattice period in the same St20 steel in the normalized state, this being attributable to the high carbon content in the martensite lattice.

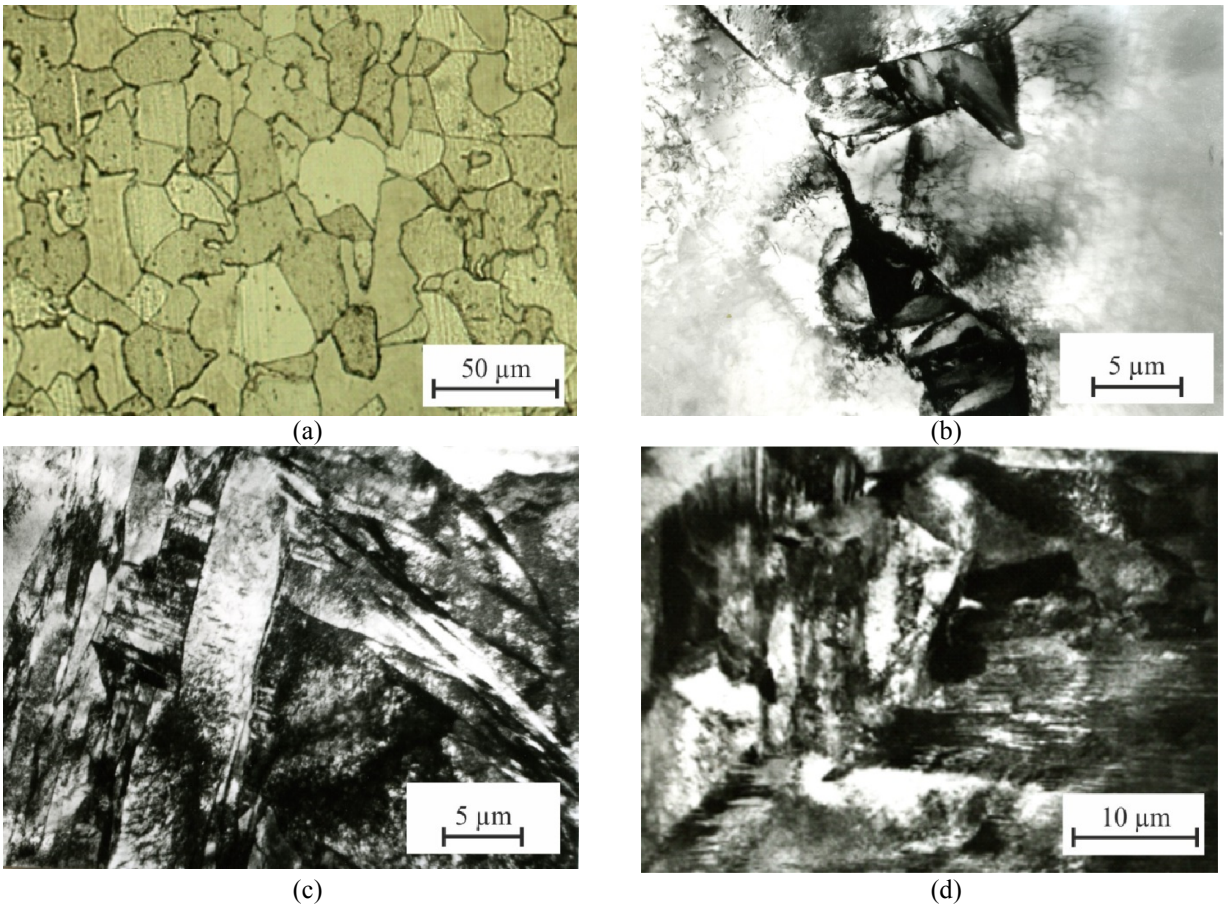

FIGURE 2. The microstructure of the St20 steel after stepwise quenching under the following conditions: T_a = 860 °C (30 min) + T_{oc} = 680 °C (20 min) + water cooling

The ~40% greater physical widening of the 110 and 222 interference lines in the X-ray diffraction pattern of the specimen quenched from 900 °C as compared to that of the specimen quenched from 860 °C testifies that a decrease in austenization temperature causes a decrease in the dislocation density and the level of microstresses by about the order of magnitude.

In the X-ray diffraction pattern of the specimen after stepwise quenching, the 110 interference maximum consists of a sharp high peak smeared towards smaller Wolf-Bragg angles (Fig. 3). On the basis of the electron microscopy data, this can be interpreted as follows. The 110 reflection is the superposition of the 110 lines of ferrite, martensite, and bainite; the smearing of the interference maximum towards smaller Wolf-Bragg angles is due to reflection from

the (101) and (011) planes of tetragonal martensite having a wide range of the period ratio c/a. The area of the 101-011 lines of martensite is ~25% of the area of the 110 line, although for martensite the ratio of the integral intensity of the 110m and 101m+011m lines is 1:2 [13]. Obviously, this is due to a relatively small amount of tetragonal martensite in the specimen under study.

A wide spectrum of martensite tetragonality (a wide range of carbon content in the martensite lattice) is caused by the inhomogeneity in terms of carbon acquired under low-temperature heating for quenching followed by overcooling. The calculation of the periods a along the 110 line and c over the minimum and maximum Wolf-Bragg angles of the 101-011 line yields the following values: a = 2.868 Å (0.2868 nm), c = 2.918–3.003 Å (0.2918–0.3003 nm), c/a = 1.02–1.05.

According to the found values of c/a and equation (1), the carbon content in the martensite, and hence in the austenite from which it has formed, is p = 0.5–1.2 wt%. This indicates the depth of carbon-enrichment of austenite microvolumes and the spread of carbon content during stepwise quenching.

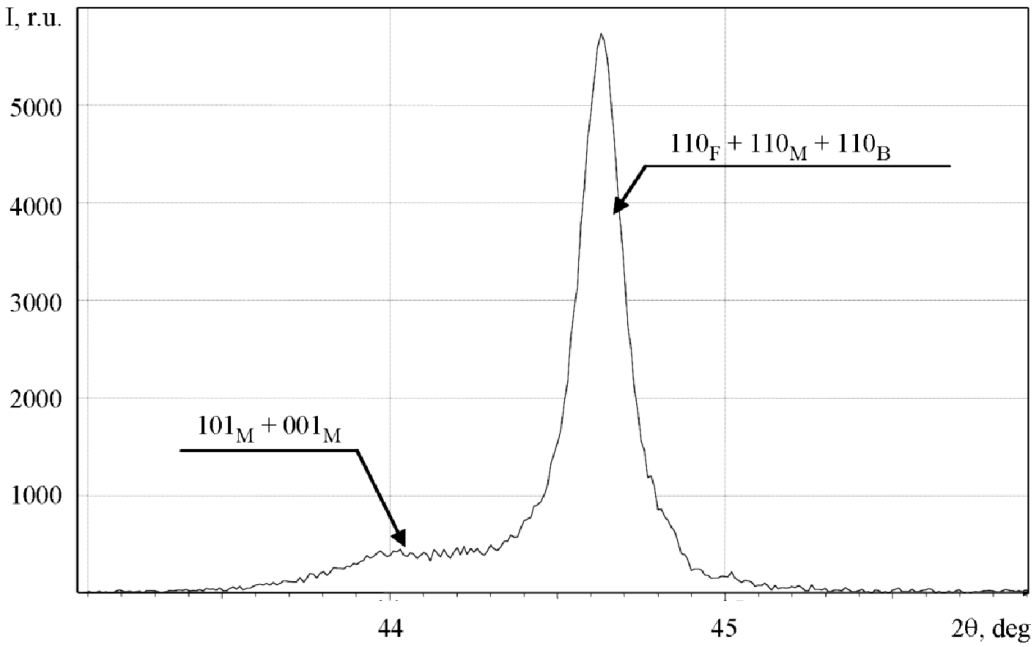

FIGURE 3. A fragment of the X-ray diffraction pattern for the stepwise-quenched St20 steel

Another feature of the X-ray diffraction pattern of the specimen treated by stepwise quenching is the absence of physical widening 222, though it reaches 0.01695 and 0.00931 rad for the specimens quenched from 900 and 860 °C, respectively. This is attributable to deep compensatory relaxation of internal stresses in the stepwise-quenched specimen [15]; namely, the stresses resulting from shear transformation products (martensite + bainite) are compensated by stresses of the opposite sign in a soft "jacket" of previously precipitated ferrite, due to the emergence of a dislocation ensemble in it. These high-density dislocations are detected electron-microscopically in excess ferrite (Fig. 2b).

Thus, the combination of high strength and ductility in the stepwise-quenched St20 results from the formation of a unique microstructure consisting of "grains" of the strengthening phase with shear transformation products (from lower bainite to high-carbon tetragonal martensite) and grains of ferrite with high dislocation density, with the elastic stress fields compensating the stresses caused by the formation of martensite and bainite. The share of the strengthening phase is ~45%.

After quenching, both steels have a high level of strength properties with rather low ductility, especially if one judges by $\sigma_{0.2}/\sigma_u$ and uniform elongation δ_{un} (Table 1). The situation is opposite in the normalized state, namely rather low strength with high ductility.

TABLE 1. The mechanical properties of the St20 and 09G2S steels

Steel	τ_{oc}, min (T_{oc} = 680 °C)	Heat treatment	HV	σ_u, MPa	$\sigma_{0.2}$, MPa	$\sigma_{0.2}/\sigma_u$	δ_{tot}, %	δ_{un}, %
St20	–	quenching	310	1355	1131	0.83	7	2
	20	stepwise quenching	265	669	400	0.60	22	14
	–	normalization	134	413	259	0.63	42	28
09G2S	–	quenching	334	1168	972	0.83	13	3
	5	stepwise quenching	258	760	460	0.60	21	12
	–	normalization	162	491	359	0.73	26	15

In this respect, the advantages of stepwise quenching are obvious. Ensuring enhanced (by $\sigma_u \approx 260$ MPa and $\sigma_{0.2} \approx 100$ MPa) strength properties as compared to the normalized state, it provides the level of plasticity required by GOSTs for hot-rolled products (sheets, shapes, pipes, etc.) made from low-carbon steels ($\delta_{un} \geq 12$–14%). Herewith, the strength properties of the 09G2S steel exceed a little those of the St20 steel, the level of plasticity being practically the same. This reveals another feature of TFMSs implying that high structural strength in them is reached with lower carbon content and without adding expensive alloying elements.

CONCLUSION

1. Stepwise quenching with austenization at T_a = 860 °C (30 min), overcooling to T_{oc} = 680 °C with 20 min soaking for the St20 steel and 5 min soaking for the 09G2S steel forms a high complex of mechanical properties of the St20 steel (σ_u = 669 MPa, $\sigma_{0.2}$ = 430 MPa, δ_{tot} = 22%, and δ_{un} = 14%) and the 09G2S steel (σ_u = 760 MPa, $\sigma_{0.2}$ = 460 MPa, δ_{tot} = 21%, and δ_{un} = 12%).
2. The strengthening phase "grains" sized ~20 μm contain a spectrum of shear transformation products from lower bainite crystals to low-temperature martensite with ~100 Å thick microtwins and ~35 μm grains of ferrite with high density of dislocations, whose elastic stress fields compensate the stresses caused by martensite and bainite formation. The degree of martensite tetragonality reaches c/a = 1.02–1.05.
3. The soft component of the heterophase structure consists of grains of ferrite containing high density of dislocations, whose elastic stress fields deeply compensate the stresses arising during the formation of martensite and bainite.
4. It is expedient to use stepwise quenching under the proposed conditions as the final heat treatment of products (sheets, shapes, or pipes) manufactured by hot rolling.

ACKNOWLEDGMENTS

The work was done within the state order of the government assignment for IES UB RAS, theme No. AAAA-A18-118020790141-2 (0391-2018-0008 project 18-11-1-11). Tests were performed in the "Plastometriya" collective use center of the Institute of Engineering Science UB RAS.

REFERENCES

1. S. A. Golovanenko and N. M. Fonshtein, *Two-Phase Low-Alloy Steels* (Metallurgiya, Moscow, 1986).
2. B. M. Bronfin, M. I. Goldshtein, and V. P. Shveikin, Izv. AN SSSR, Metally **1**, 127–133 (1987).
3. I. Yu. Pyshmintsev, *Hardening of Sheet Steels for Cold Forming* (AMB, Ekaterinburg, 2004)
4. S. V. Grachev, V. R. Baraz, V. P. Bogatov, and V. P. Shveykin, *Physical Metallurgy*: a Textbook for High Schools, 2nd ed. (UGTU-UPI Publ., Ekaterinburg, 2009).
5. Yu. D. Morozov et al., Metallurgist 1, 21–28 (2008).

6. M. A. Smirnov, V. M. Schastlivtsev, and L. G. Zhuravlev, *Fundamentals of Heat Treatment of Steel*: a Tutorial (UrO RAN Publ., Ekaterinburg, 1999).
7. G. V. Kurdyumov, L. N. Utevsky, and R. I. Entin, *Transformations in Iron and Steel* (Nauka Publ., Moscow, 1977).
8. K. N. Sokolov and I. K. Korotich, *Technology of Heat Treatment and Design of Heat-Treating Departments*: Textbook (Metallurgiya Publ., Moscow, 1988).
9. V. M. Farber, "Methods for increasing the structural strength of pipes," in *Achievements in the Theory and Practice of Pipe and Tube Production*: Collection of Papers (UGTU-UPI Publ., Ekaterinburg, 2004), pp. 390–394.
10. R. G. Davies, Metallurgical Transactions A **9A** (5), 671–679 (1978).
11. V. I. Izotov and N. I. Khandarev, The Physics of Metals and Metallography **34** (1), 123–132 (1972).
12. V. M. Schastlivtsev, The Physics of Metals and Metallography **38** (4), 793–802 (1974).
13. Ya. S. Umansky et al., *Crystallography, Radiography, and Electronic Microscopy* (Metallurgiya Publ., Moscow, 1982).
14. S. S. Gorelik, Yu. A. Skakov, and L. N. Rastorguev, *X-Ray and Electron-Optical Analysis*: a Tutorial for High Schools, 4th ed. (MISIS Publ., Moscow, 2002).
15. V. M. Farber, O. V. Selivanova, Metally **1**, 110–115 (2001).
16. V. M. Farber, The Physics of Metals and Metallography **76** (2), 35–40 (1993).
17. A. P. Gulyaev, *Physical Metallurgy*: a Textbook for High Schools, 6th ed. (Metallurgiya Publ., Moscow, 1986).
18. I. I. Novikov, *Theory of Heat Treatment of Metals*: a Textbook for High Schools, 4th ed. (Metallurgiya Publ., Moscow, 1986).
19. V. G. Sorokin and M. A. Gervasyev, "Studying the complex of mechanical properties of cold-resistant pearlite-reduced steels," in *Advanced Methods for Surface and Volumetric Hardening of Critical Parts in Mechanical Engineering* (TsNIITyazhMash Publ., Moscow, 1992), pp. 18–24.